Gene Expression **2023** vol. 000(000) | 000–000 Epub
DOI: 10.14218/GE.2023.00043

Original Article

Detailed Stability and Unfolding Study of *Mycobacterium* Global Transcription Regulator Protein

Abinit Saha[1,2#], Devlina Chakravarty[3#] and Soumyananda Chakraborti[1,4,5*]

[1]*Department of Biochemistry, Bose Institute, Kolkata, India;* [2]*Adamas University, Barasat-Barrackpore Road Jagannathpur, Kolkata, India;* [3]*Department of Chemistry, Rutgers University, Camden, USA;* [4]*Malopolska Centre of Biotechnology, Jagiellonian University, Krakow, Poland;* [5]*National Institute of Malaria Research, New Delhi, India*

Received: June 17, 2023 | **Revised:** July 27, 2023 | **Accepted:** November 08, 2023 | **Published online:** December 14, 2023

Abstract

Background and objectives: The cyclic adenosine monophosphate Receptor Protein of *Mycobacterium tuberculosis* (CRP_{Mt}) (*Rv3676*), is a global transcriptional regulator and plays a pivotal role in the survival and infection of *Mycobacterium*. This signaling protein (CRP_{Mt}) shares several common structural and functional features with the CRP from *Escherichia coli*. Structurally, CRP_{Mt} is a homodimer that undergoes allosteric changes upon cyclic AMP binding. This binding also triggers the activation of several genes responsible for various physiological processes in this bacterium. Despite the importance of CRP for *mycobacterial* survival, limited information is available regarding the stability and unfolding properties of the protein. The main objective of this study is to study stability, unfolding and dynamics of CRP_{Mt} in terms of its structure.

Methods: In this study, we monitored the stability and unfolding of CRP_{Mt} using various biophysical and computational techniques.

Results: We experimentally studied protein unfolding in the presence of chemical denaturants [urea and guanidine hydrochloride (GdnHCl)]. The results from these chemical-induced unfolding studies suggest that CRP_{Mt} follows a two-state transition and that chemical-induced protein denaturation is reversible. According to circular dichroism and activity data, CRP_{Mt} structure and function were restored upon refolding. We also studied the stability and unfolding of the CRP_{Mt} protein against temperature variations and protease action (trypsin). Limited proteolysis experiments provide insights into the minimum domain structure requirement for CRP_{Mt} activity. Interestingly, temperature-induced CRP_{Mt} unfolding was completely different compared to chemical-induced unfolding. The thermal unfolding of CRP_{Mt} was found to be irreversible, leading to the formation of insoluble aggregates at elevated temperatures. To understand why the thermal unfolding of the protein differed from chemically induced unfolding, we carried out a detailed molecular dynamics simulation analysis of the protein at three different temperatures. The results from these molecular dynamics simulations mechanistically validate the significant differences between chemical and temperature-induced CRP_{Mt} unfolding.

Conclusion: Our study provides detailed insights into the stability and folding/unfolding properties of CRP_{Mt}, which could be useful in developing new anti-mycobacterial medicines.

Keywords: *Mycobacterium tuberculosis* transcription regulation protein; Protein unfolding; Fluorescence and circular dichroism spectroscopy; Proteolysis; Molecular dynamic simulation.

Abbreviations: ANS, 8-anilino-1-napthalenesulphonate; cAMP, cyclic adenosine monophosphate; CD, circular dichroism; CRP_{Mt}, cyclic adenosine monophosphate receptor protein of *Mycobacterium tuberculosis*; CRP, c-AMP receptor protein; EMSA, electrophoretic mobility shift assay; far-UV, far-ultra violet; FNR, fumarate, and nitrate reduction regulatory protein; GdnHCl, guanidinium chloride; IPTG, isopropyl β-D-thiogalactopyranoside; KI, potassium iodide; M, molarity; MD, molecular dynamics; PCR, polymerase chain reaction; RMSD, root mean square deviation; RMSF, root mean square fluctuation; SDS–PAGE, sodium dodecyl sulfate-polyacrylamide gel electrophoresis; SEC, size-exclusion chromatography.

***Correspondence to:** Soumyananda Chakraborti, National Institute of Malaria Research, Dwarka Sector 8, New Delhi 110077, India. ORCID: https://orcid.org/0000-0002-7384-690X. Tel: +91-9354652349, Fax: +91-11-278530116. E-mail: soumyabiochem@gmail.com

[#]These authors contributed equally to this study.

How to cite this article: Saha A, Chakravarty D, Chakraborti S. Detailed Stability and Unfolding Study of *Mycobacterium* Global Transcription Regulator Protein. *Gene Expr* 2023;000(000):000–000. doi: 10.14218/GE.2023.00043.

Introduction

Mycobacterium tuberculosis is highly pathogenic, and its infection causes tuberculosis, contributing to approximately 2 million deaths per annum.[1] *M. tuberculosis* is a highly adaptable bacterium that can persist in a non-replicating state for a long time when the environment is unfavorable. It is a successful pathogen that can modulate its host immune response to survive without adversely affecting the host immune system.[2,3] Interestingly, one-third of the world's population is believed to be infected by *Mycobacterium tuberculosis*.[1] Cyclic adenosine monophosphate (cAMP) is a vital

signaling molecule in *M. tuberculosis*. It also plays a crucial role in altering the host immune system at the time of infection.[4,5] Intriguingly, the adaptability of the cAMP-binding domain has evolved in such a way that it can perform diverse physiological functions in response to a broad range of signals,[6–8] with the best and the most studied prototype proteins of this family being c-AMP receptor protein (CRP) and fumarate and nitrate reduction regulatory protein (FNR) of *E. coli*, which are known to control genes in hypoxia and starvation, respectively.[7]

Mycobacterium tuberculosis H37Rv also has a CRP/FNR homolog, CRP_{Mt} (*Rv3676*) the protein is encoded by the gene *rv3676*.[9] It is also important to note that this gene (*rv3676*) is present in almost all sequenced mycobacterium genomes. It has also been reported that this protein is a highly branched member of the CRP and CooA family of proteins.[7,8] Protein sequence analysis revealed that CRP_{Mt} is 53% similar and 32% identical to its *E. coli* homolog.[10]

Similar to *E. coli* CRP, CRP_{Mt} also exists as a homo-dimmer. Structurally CRP_{Mt} carries two domains, and the cAMP-binding occurs at the N-terminal domain (residues 1–114) whereas the C-terminal domain (146–223) consists of mainly the DNA-binding helix turn helix motif. These two domains are connected by a hinge region (a helix between residues 117–144 mainly anchors these hinge regions). This helix forms the majority of the intersubunit interactions. The details of domain topology are shown in Figure S1. However, unlike *E. coli* CRP, *CRPMt* carries three additional short helices and a hairpin-like structure in the N-terminal domain (residues 54–73) that are absent in *E. coli* CRP.[11] Detail structural investigation also reveals that the N-terminal domain of *CRPMt* possesses more beta-sheet structure compared to C-terminal domain. Although CRP_{Mt} is a cAMP-binding transcriptional regulator, it is interesting to note that cAMP-binding to CRP_{Mt} is associated with minimal structural rearrangements in comparison to *E. coli* CRP.[11–13]

Moreover, it has also been reported that deletion of this protein, *i.e.*, CRP_{Mt} may lead to impaired growth in bone marrow-derived macrophages in a laboratory medium and delayed bacterial growth in a mouse model system.[10,14,15] Thus, it is imperative to note that this global transcriptional factor, *i.e.*, CRP_{Mt} might have played a significant role in the survival of this particular pathogenic bacterium, especially in macrophages. Although the physiological importance, function, and structural detail of this protein are well established, little is known about its stability and folding mechanism.

Protein folding is an essential physical process by which a nascent polypeptide chain folds into proper three-dimensional functional forms. Though this process is of the greatest importance, how it is completed (protein folding and unfolding) is only partially understood.[16,17] Thus, a detailed study of the protein folding mechanism is very important.[18–20] Unlike single-domain proteins, oligomeric multi-domain proteins usually fold by multiple-step processes involving the formation of one or more meta-stable intermediates. Thus, it is crucial to identify and characterize these intermediate conformations to understand the mechanism of protein folding. Equilibrium denaturation is one of the valuable methods to understand the structure, stabilization, and folding of a protein, and protein folding can be easily tracked by the characterization of its intermediates both *in vitro* and *in vivo*.[21,22] Chemical denaturant such as urea or guanidinium chloride (GdnHCl) is commonly used for equilibrium unfolding of the protein and intermediate charecterization.[23]

In this study, we explored the structural and functional changes of CRP_{Mt} associated with the GdnHCl and urea-induced unfolding using various spectroscopic techniques such as tryptophan fluorescence spectroscopy, 8-anilino-1-napthalenesulphonate (ANS) fluorescence, and circular dichroism (CD), *etc*. These methods were used to study the changes in the tertiary and secondary structure of CRP_{Mt} during denaturant-induced unfolding. Size exclusion chromatography is further used to monitor the purity and oligomerization state of the protein. Furthermore, the refolding of CRP_{Mt} to its native form and restoration of activity was also explored by the withdrawal of both denaturants. Restoration of the protein structure was examined by spectroscopic and gel filtration profiles of refolded protein. The restoration of the individual domain structure was verified by partial digestion of the protein with trypsin followed by visualization of the tryptic digest fragments by running sodium dodecyl sulfate-polyacrylamide gel electrophoresis (SDS–PAGE) gel (13%). DNA binding activity of the protein was also examined by Electrophoretic mobility shift assay (EMSA). These studies confirm restoring the CRP_{Mt} structure and the activity upon refolding.

We further investigated the temperature-induced unfolding of CRP_{Mt} by measuring the light scattering of the protein. We observed that the protein forms visible aggregates at higher temperatures (65°C), indicating irreversible unfolding of the protein. To understand the effect of increasing temperature on CRP_{Mt} structure, we performed extensive molecular dynamics simulations of the protein under normal conditions (25°C) and compared the dynamics at 45°C and 65°C.

We found that destabilization of the structure occurs at specific regions due to high temperatures, with unfolding starting at the terminal region first and then at the interface. Moreover, secondary structural elements, hydrogen-bonding patterns, and the interface are significantly affected at higher temperatures. Interestingly, a strong correlation was observed between our experimental results and simulations, further validating our findings. Given that CRP_{Mt} is a global transcriptional regulator, it could potentially be used as a drug target. In this proteomics era, understanding the structure-function relationships of target proteins is crucial for designing target-specific drugs.

Materials and methods

Materials

8-anilino-1-napthalenesulphonate (ANS) and glutaraldehyde were purchased from Sigma Chemical Company, USA. Analytical gel-filtration column (SuperdexTM 75 HR 10/30) and protein molecular weight standards were obtained from GE Healthcare Bio-Sciences AB, Sweden (formerly Amersham Biosciences). Radioactive [γ-32P] adenosine triphosphate was obtained from the Board of Radiation and Isotope Technology, India. Oligonucleotides were custom-synthesized from MWG-Biotech AG, Germany, or Sigma-Genosys, USA. All other chemicals obtained from Merck were analytical grade. All enzymes used for DNA manipulation were procured either from the United States Biochemical Corp (USA), Promega Biosciences (USA), or Roche Applied Sciences (Germany). Thrombin was purchased from Novagen® Biosciences. The expression vector used for this study was pET28a (+) (Novagen). XL1 Blue and BL21 (DE3) were used for cloning purposes. All these strains were maintained as glycerol stocks at −80°C.

Cloning, overexpression, and purification of CRP_{Mt}

CRP_{Mt} was cloned directly from the *Mycobacterium tuberculosis* genomic DNA using ABS1 primers (forward primer) and ABS2

Table 1. C_m values from different unfolding assays

Protein	Assay Type	Denaturant	C_m (M)
CRP_{Mt}	far-UV CD	Urea	4.49 ± 0.02
CRP_{Mt}	Trp-fluorescence	Urea	4.10 ± 0.02
CRP_{Mt}	far-UV CD	GdnHCl	1.94 ± 0.02
CRP_{Mt}	Trp-fluorescence	GdnHCl	1.29 ± 0.01

CD, circular dichroism; CRP_{Mt}, cyclic adenosine monophosphate receptor protein of *Mycobacterium tuberculosis*; far-UV, far-ultra violet; GdnHCl, guanidinium chloride; M, molarity.

(reverse primer). The sequence of primers that were used to amplify the CRP_{Mt} gene was mentioned in Table 1. The purified restriction enzyme-digested PCR product was ligated into the *Eco*RI and *Xho*I-digested pET28a plasmid, which was used to transform competent *E. coli* XL1B cells. Plasmid DNA from selected clones with an N-terminal hexa-histidine tag was isolated and transformed into *E. coli* BL21 cells for protein expression. Expression of CRP_{Mt} was induced by the addition of 0.5 mM isopropyl β-D-thiogalactopyranoside (IPTG) to an *E. coli* BL21 cell culture when the cell culture OD_{595} reached 0.5 after the addition of IPTG cells were grown further for 3 h at 37°C. Finally, cells were harvested and suspended in sonication buffer [20 mM sodium phosphate buffer pH-7, 500 mM NaCl, and 10% glycerol] and then subjected to sonication and centrifugation. After sonication, the pellet was discarded, and the supernatant was collected and loaded into a pre-equilibrated nickel agarose resin (Qiagen), which had been equilibrated in sonication buffer and washed sequentially with wash buffers containing 10 and 50 mM of imidazole. The protein was finally eluted in 500 mM imidazole-containing buffer, and the purity of the protein was checked by nanodrop and running the protein on a 12.5% SDS-PAGE (Figure S2). Figure S2 shows the purification profile of the 6x His-CRP_{Mt} protein. Imidazole was dialyzed with dialysis buffer [20 mM Tris-Cl (pH-7.5), 150 mM NaCl, 5 % Glycerol, and 1 mM EDTA].

Size-exclusion chromatography

Size-exclusion Chromatography experiments were performed in an ÄKTA™ FPLC system (Amersham Biosciences, Sweden) connected to a Superdex®75 HR or Superdex®200 HR column using the protocol developed by Datta et al.[24] At a time of purification, 250–500 µg of the protein (recombinant *CRPMt* or a standard marker protein) was applied to the column. Before loading the protein, the column was pre-equilibrated with buffer A [20 mM Tris-Cl (pH 7.5), 150 mM NaCl, 5% Glycerol, and 1 mM EDTA]. All experiments were performed in buffer A unless stated otherwise. A fixed flow rate of 0.5 mL/min was maintained throughout the process. The Rf (Retardation Factor) value was calculated according to the following equation,

$$Rf = \frac{Ve - V_0}{Vt - V_0}$$

in the equation, Ve = Elution volume; V0 = Void volume, and Vt = Total volume of the column.

To understand the underlying mechanism involved in the folding process of this protein in the presence of chaotropic agents, the protein was first denatured at different concentrations of urea or GdnHCl overnight at 4 °C and then applied to the column. The gel filtration column was equilibrated with the respective denaturant-containing buffer solutions before loading the proteins.

Circular dichroism (CD) spectroscopy

Circular Dichroism (CD) measurements were also carried out using the protocol developed by *Datta et al.*[24] Briefly, CD spectroscopy was performed at room temperature using a JASCO J600 spectropolarimeter equipped with a temperature controller. Far-ultra violet (Far-UV) CD (260–200 nm) was recorded using a cuvette of 1 mm path length and 10 µM protein solution for each measurement. To study the effects of denaturants on the secondary structures of proteins, far-UV CD spectra (215–260 nm) of urea and GdnHCl-treated samples were recorded individually. The sample was prepared by incubating the protein with an increasing concentration of urea/GdnHCl for 18 h at 4°C. Protein concentrations were kept at 10 µM for all far-UV CD measurements, and experiments were performed in triplicate. Each measurement was a signal average of five spectral scans to maximize the signal-to-noise ratio. The buffer contributions were also subtracted from the corresponding spectra of protein samples. The CD results were finally expressed regarding mean residual ellipticity.

Tryptophan fluorescence spectroscopy

Fluorescence spectroscopy was used to study the unfolding/refolding behavior of CRP_{MT} induced by chaotropic agents (urea and GdnHCl). All measurements were carried out using a Hitachi F3000 spectrofluorometer with 10 µM protein. Fluorescence was measured by tryptophan excitation at 295 nm and emission at 310–400 nm with excitation and emission bandpass of 5 nm.[22] The equilibrium unfolding experiments were performed after incubating the protein with an increasing concentration of urea/GdnHCl for 18 h at 4°C. Finally, the unfolding of CRP_{MT} was measured by observing the changes of fluorescence λ_{max} as a function of urea/GdnHCl concentration. 8-Anilinonaphthalene-1-sulfonic acid (ANS), a highly hydrophobic fluorescence dye, is generally used to track the hydrophobic exposure of protein during the unfolding/folding process.[22] For ANS fluorescence measurement, the excitation wavelength was set at 340 nm, and the emission spectra were recorded at 440–600 nm range. The experiments were carried out in triplicate at room temperature. For almost all experiments, fluorescence intensities were determined at the λ_{max} after inner filter correction.[25] The inner filter effect is a prevalent problem in fluorescence measurement studies. The primary reason for the inner filter effect is the absorption of light by any fluorophore (protein).[26]

Analysis of unfolding curves

Assuming that the unfolding of CRP_{Mt} follows a two-state unfolding, the fraction of unfolded protein molecules (f_u) was calculated from the following equation[27]:

$$f_u = \frac{X_n - X}{X_n - X_u}$$

where X, X_n, and X_u represent the observed spectroscopic signal at any particular denaturant concentration, the spectroscopic signal in the completely folded state, and the spectroscopic signal in the completely denatured state, respectively. The C_m (denaturant concentration at the midpoint of unfolding transition) value was determined by nonlinear fitting of the unfolding data to the following equation using the software as described previously.[28]

$$Y = \text{bottom} + \frac{\text{top} - \text{bottom}}{1 + 10^{X-Cm}}$$

In the above equation, X and Y are the concentration of the unfolding agent and the fraction of unfolded protein molecules, respectively.

Acrylamide and potassium iodide (KI) quenching of tryptophan residue

Quenching of tryptophan fluorescence of CRP_{Mt} by acrylamide and potassium iodide (KI) was also monitored at room temperature using a Hitachi F3000 spectrofluorometer. For measurement, 4 µM of protein solution was used, protein excitation was performed at 295 nm, and the data was recorded at the fixed emission wavelength of 340 nm in the presence of different concentrations of the quencher (acrylamide or KI) added in small volumes from a concentrated (2 M) stock solution. Band passes of 5 nm were used on both sides. The total reaction volume was set to 1 mL.

Refolding of denatured proteins

To study the refolding of CRP_{Mt}, the protein was denatured either with 7 M urea or 5 M GdnHCl. The unfolded protein was subjected to dialysis overnight against buffer A (with at least two changes in the buffer) at 4°C to completely remove all the denaturants. Refolded protein (10 µM) was used for both CD and fluorescence measurements. To confirm the complete refolding of CRP_{Mt} domains, refolded CRP_{Mt} (15 µg) along with native CRP_{Mt} (15 µg) were digested by 0.2 µg trypsin for different periods followed by the analyses of the fragments by a tris-tricine SDS-PAGE.

Thermal aggregation

The thermal aggregation of CRP_{Mt} (10 µM in buffer A) was studied to understand its aggregation rate. This was done by monitoring light scattering at 360 nm using a spectrofluorometer (Hitachi F-3000), as described by previous research.[24] The wavelength and bandpass were set at 360 nm and 5 nm, respectively, for both excitation and emission. The protein solution within the cuvette chamber was heated to the desired temperature using a water-bath temperature controller (NesLab Inc.) and equilibrated for 4 min before individual readings were taken.

Construction of reporter gene plasmids

The region of the DNA sequence upstream of rpf A was generated using polymerase chain reaction (PCR) from *M. tuberculosis H37Rv* genomic DNA using the primer pairs (Table S1). The PCR product (200-bp) was then cloned into a pBluescript vector at the *Eco* RV site to obtain the plasmid pABS 04.

Preparation of DNA fragments containing pWhiB1 region of M. tuberculosis

DNA fragments used in this work were derived from the plasmid pABS 04 by PCR amplification using suitable primers (rpf A forward and reverse primer, Table S1). These fragments were further purified by running on a 1% agarose gel, cut out from the gel, and final purification was made using a Qiagen Gel Extraction Kit. The final concentration of the DNA was estimated from its absorbance at 260 nm. The PCR products containing the promoter/operator regions were end-labeled with [γ-^{32}P] adenosine triphosphate and T4 polynucleotide kinase for 1 h at 37°C. The labeled product was then purified through a Qiagen Gel Extraction Kit.

Electrophoretic mobility shift assays (EMSA)

Radiolabeled DNA (~5 ng) was incubated with 0–20 µM CRP_{Mt} or its mutants in the presence of 20 mM HEPES (pH 7.5), 0.2 mM EDTA, 10 mM $(NH_4)_2SO_4$, 1 mM dithiothreitol, 15 mM $MgCl_2$, 15 mM KCl and 0.05 mg/mL bovine serum albumin, for 30 minutes at 25°C. The resulting complexes were then separated on 6 % polyacrylamide gels buffered with 0.5 X TBE (45 mM Tris borate, 1 mM EDTA). Gels were typically run at 16 V/cm for 2–3 h to obtain the optimum separation and dried and autoradiographed.[29]

Crystal structure of CRP

The starting structure for our simulations was taken from the protein data bank [crystal structure of CRP from *Mycobacterium tuberculosis*; PDBID: 3H3U, chains A and B)].[12] The structure had missing residues in both subunits [chain A (1, 14–17, 24–26) and in chain B (215–224)]. The missing residues were filled using the PDBSEQRES record (from the PDB header section) and Modeller (https://salilab.org/modeller/).[30]

Molecular dynamics (MD) simulation

All simulations were performed using the Gromacs molecular dynamics (MD) package,[31] in explicit solvent, using the Optimized Potential for Liquid Simulations AA/L all-atom force field.[32] Solvent molecules were described by the extended simple point charge model. Electrostatic interactions were implemented using Particle mesh Ewald. The temperature bath was set up with the Berendsen thermostat at 300 K for the control and at higher temperatures 318 and 338 K, the time step was set to 2 fs, and bonds involving hydrogens were constrained.[33] We have used a dodecahedron box for the CRP_{MT} system. The details of the simulations performed are listed in Table S2. Analyses of the trajectories were performed using Gromacs analysis tools, and all plots were generated using matplotlib [https://matplotlib.org/3.2.0/index.html], figures of structures were generated using PYMOL [https://pymol.org/2/].

Results

GdnHCl and urea-induced unfolding of CRP_{Mt}

Far-UV CD was used to study the unfolding of CRP_{Mt} in the presence of both urea and GdnHCl. CD analysis provides essential information regarding the change in secondary structures of the protein. Among different secondary structures, the α-helix structure in the protein shows strong signals at 222 nm, and any decrease in the value of the signal is normally associated with a decrease in the helical content of the protein. CRP_{Mt} is mainly an α-helical protein (as the protein consists of ~37% α-helices), so by extracting the θ_{222} values from the CD spectra of the protein (Fig. 1a and b) and plotting these values against the corresponding denaturant concentrations, one can easily get information about CRP_{Mt} folding/unfolding behavior. According to our data, CRP_{Mt} shows monophasic unfolding curves in the presence of both denaturants (Fig. 1a and b). The unfolding CRP_{Mt} in the presence of GdnHCl starts around 1 M and completes at 4 M; in the case of urea, *CRPMt* unfolds at 3.5 M, and denaturation completes at 6 M. The unfolding behavior of CRP_{Mt} follows the general trend of any globular protein. We have found that CRP_{Mt} is denatured early in the presence of GdnHCL (GdnHCL is always considered a much stronger denaturing agent than urea).[34] The intrinsic tryptophan fluorescence intensity values were collected from (Fig. 1c and d) and plotted against the increasing GdnHCl/urea concentrations. In the case of Trp fluorescence, the curves were also roughly monophasic, and the unfolding profile of the protein was very similar to what we observed before with CD spectroscopy. So, it can be suggested that the unfolding of CRP_{Mt} in the presence of denaturant (GdnHCl and urea) follows a two-state model without any detectable intermediate. The calculated C_m (denaturant concentration at the midpoint of unfolding transition) values from different experiments were provided in Table 1. We have also studied CRP unfolding in the presence of c-AMP by fluorescence and CD spectroscopy as CRP is

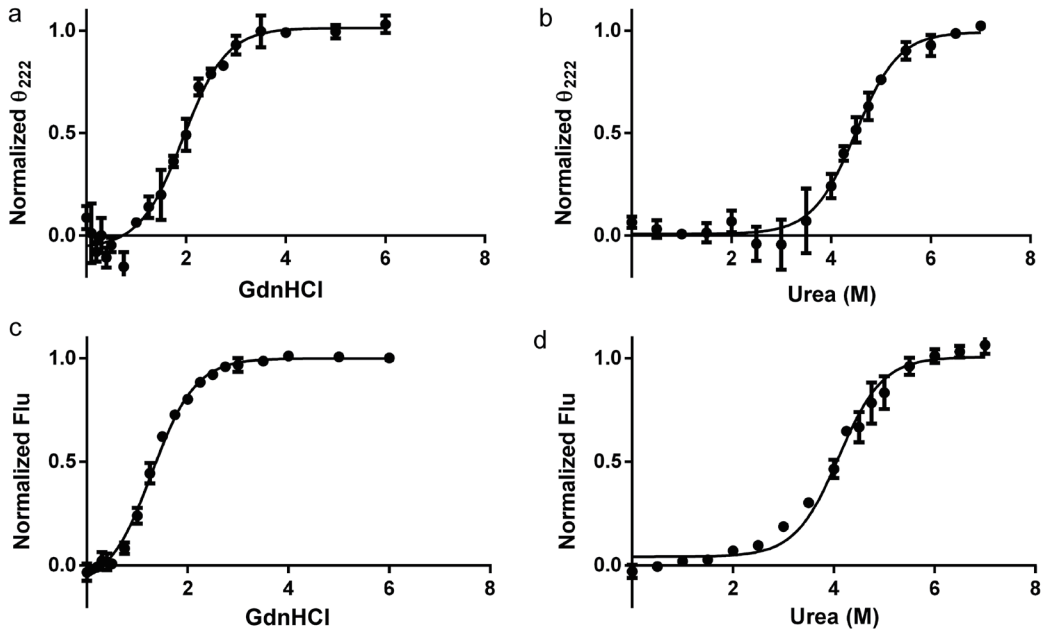

Fig. 1. Urea and GdnHCl induced equilibrium unfolding of *CRP$_{Mt}$* measured by circular dichroism and fluorescence. The θ_{222} (ellipticity at 222 nm) values, derived from the recorded far-UV CD spectra of a protein in the presence of GdnHCl (a), and urea (b) were normalized concerning that of the same protein in the absence of any chemical denaturant. The plots of normalized θ_{222} values vs. urea and GdnHCl concentrations indicate the alternation of secondary structure (particularly α-helix) of the protein samples at increasing urea and GdnHCl concentrations. Similarly, intrinsic Trp fluorescence intensity values (Flu) at 334 nm were determined from the fluorescence spectra, normalized (as above), and plotted against increasing GdnHCl (c) and urea (d) concentration. From the images, it was evident that the protein was more resistant towards urea compared to GdnHCl. CD, circular dichroism; *CRP$_{Mt}$*, cyclic adenosine monophosphate receptor protein of *Mycobacterium tuberculosis*; far-UV, far-ultra violet; GdnHCl, guanidinium chloride; M, molarity.

switching its function by binding with cyclic-AMP. Protein unfolding was induced by either urea or GdnHCl. Our data reveals that c-AMP stability and unfolding of *CRPMt* remain unaltered compared to the wild-type protein (Fig. S3). Our data further suggests that c-AMP binding is not causing any significant change in the *CRPMt* structure or global conformation change of the protein.

Quenching of tryptophan fluorescence

The tryptophan fluorescence of proteins decreases in the presence of molecules like acrylamide or potassium iodide (KI), and they are known as quenchers. The quenching phenomenon can also be used to probe the accessibility of tryptophan residues in a protein. *CRP$_{Mt}$* has two tryptophan residues, viz. trp112 and trp 203. Tryptophan fluorescence quenching of *CRP$_{Mt}$* was studied in the presence of acrylamide and KI. The quenching data was analyzed by Lehrer plots using the following equation.[35]

$$\frac{F_0}{\Delta F} = \frac{1}{F_a}\left(\frac{1}{K_{sv}[Q]} + 1\right)$$

In the equation, F *and* F_0 represent the fluorescence in the presence and absence of quencher, and $\Delta F = (F_0 - F)$; F_a is the fraction of accessible tryptophan residues, $[Q]$ denotes the concentration of quencher and K_{sv} is the constant (also known as stern-Volmer constant) representing accessible fluorophores. From the plot of $F_0/\Delta F$ versus $1/[Q]$, the values of F_a (inverse of y-intercept) and K_{sv} (inverse of slope) can be determined. The Lehrer plots for quenching of *CRP$_{Mt}$* by acrylamide and KI are shown in Figure 2.[35] The details of parameters obtained from fittings are provided in Table 2. A value

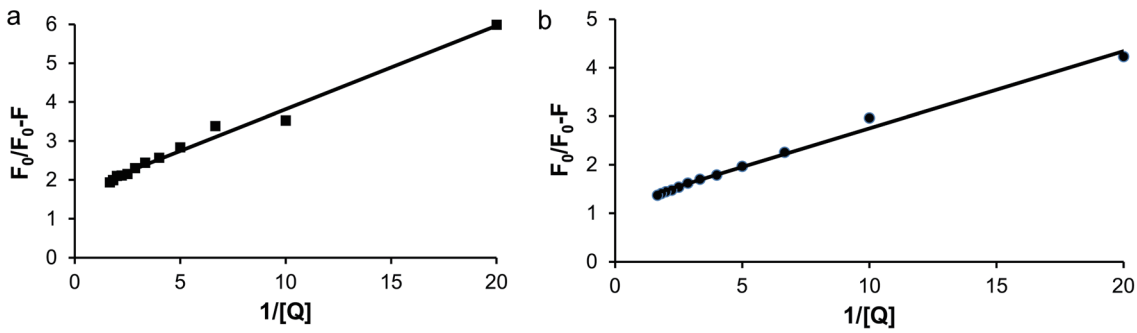

Fig. 2. Lehrer plots show tryptophan fluorescence quenching of *CRP$_{Mt}$* by two different quenchers. Quenching of tryptophan fluorescence by increasing concentration of (a) KI and (b) acrylamide. The detailed analysis of the Lehrer plot is shown in Table 2. *CRP$_{Mt}$*, cyclic adenosine monophosphate receptor protein of *Mycobacterium tuberculosis*; KI, potassium iodide.

Table 2. Fluorescence quenching data by acrylamide and KI

Quencher	y-intercept	F_a	K_{sv} (M^{-1})
Acrylamide	1.16	0.86	7.31
KI	1.67	0.59	7.89

KI, potassium iodide; M, molarity.

of about 0.86 was obtained for Fa for acrylamide quenching, indicating that both the tryptophan residues were accessible to acrylamide, with a Stern-Volmer constant of 7.31 M^{-1}. For KI, the accessibility of the tryptophan residues was only 59%. Acrylamide is a neutral quenching agent that can easily diffuse through protein structure and quench all available tryptophan residues present in CRP_{Mt}, including deeply buried tryptophan residues (trp112 and trp203). On the contrary, iodide is negatively charged and generally remains a highly hydrated molecule. As an outcome, its diffusion is minimal and only quenches tryptophan residues present at the protein surface. From quenching properties of KI and acrylamide, one can get an idea about the conformation state of the protein, and according to our analysis, in the absence of a denaturant, CRP_{Mt} almost exclusively existed in folded conformation. Although we have seen differences in quenching between acrylamide and KI, the Ksv values were low in both cases. We believe this phenomenon is attributed to the highly folded nature of CRP_{Mt} and tryptophan residues inside the core of the protein (our computational data also support this result). Due to the rigidity of the protein, acrylamide cannot penetrate deep inside CRP_{Mt} and efficiently bind tryptophan; as an outcome, low binding was observed. We have also seen increasing Ksv value of both acrylamide and KI in the presence of GdnHCl and urea (data not shown), further supporting our hypothesis.

ANS fluorescence

In the unfolding of CRP_{Mt} induced by urea and GdnHCl, the unfolding curves derived from CD and fluorescence studies did not fully align, suggesting the potential existence of an intermediate state. An ANS binding study was performed to determine whether an intermediate state of CRP_{Mt} is present during unfolding. ANS tends to bind to the hydrophobic patches of a protein that become exposed during unfolding. Typically, in the molten globule state, the hydrophobic patches of a protein are highly exposed compared to its native conformation, and ANS binds to these exposed hydrophobic patches. The binding of ANS to hydrophobic patches is directly associated with increased fluorescence intensity at approximately 490 nm. However, in our experiments with CRP_{Mt}, fluorescence intensity decreased with increasing concentrations of chemical denaturant (Fig. 3), indicating a lack of significantly exposed hydrophobic patches. Therefore, it can be concluded that the unfolding of CRP_{Mt} follows a two-state model without any notable intermediate.

Size-exclusion chromatography (SEC) of CRP_{Mt} with GdnHCl and urea

To get a complete understanding of the effect of GdnHCl and urea on the oligomerization of CRP_{Mt}, we have analyzed 0−5 M urea-equilibrated and 0−3 M GdnHCl-equilibrated CRP_{Mt} samples through SEC. Both the native and denaturant treated (Fig. 4a and b) sample shows a single peak with almost identical retention volume. According to the SEC profile, the native protein was eluted at 57.06 mL. While in the presence of varied GdnHCl concentrations (0.5, 1, 2, 2.5, and 3 M), the elution peaks were gradually shifted towards lower values (55.87, 54.01, 51.87, 49.94, and 48.96 mL) with increasing absorbance indicating subunit dissociation and unfolding. In the presence of varied urea concentrations (2, 3, 3.5, 4, and 5 M urea), the CRP_{Mt} elution profile almost follows a similar trend as of GdnHCl. Proteins were eluted at 53.43, 52.12, 51.33, 50.62, and 49.5 mL, respectively (Table 3).

Reversible unfolding of CRP_{Mt}

We were also interested in studying the reversibility of GdnHCl and urea-induced denaturation of CRP_{Mt}. We speculated that if equilibrium unfolding is reversible, CRP_{Mt} will return to its original (native) state once the denaturant is removed from the unfolding buffer. To check our hypothesis, Trp fluorescence, CD spectra and gel filtration profiles of native, likely refolded, and unfolded CRP_{Mt} were recorded (Fig. 5). All our experimental data including Trp fluorescence spectra (Fig. 5a and b), far-UV CD spectra (Fig. 5c and d) and gel filtration profiles (Fig. 5e and f) suggest restoration of its structure, once denaturant is withdrawn.

To further verify the restoration of CRP_{Mt} individual domain structures, both native CRP_{Mt} and refolded CRP_{Mt} were subjected to partial trypsin digestion followed by the visualization of the digested fragments by running samples at 13.5% SDS-PAGE. The result clearly shows that the molecular masses of all digested fragments from the refolded proteins (either generated from 5 M GdnHCl or 7 M urea) were almost similar to those prepared from the digestion of the native protein, clearly indicating genuine refolding of individual domain structure (Fig. S4).

Our previous experiments confirm the structural restoration of protein by the withdrawal of denaturant stress. In the next step, activity restoration of refolded protein was also studied by measuring the DNA binding activity of refolded CRP_{Mt}. EMSA was employed to study DNA binding activity. As evident from Figure S5, refolded CRP_{Mt}, prepared either from 7 M urea or 5 M Gdn-

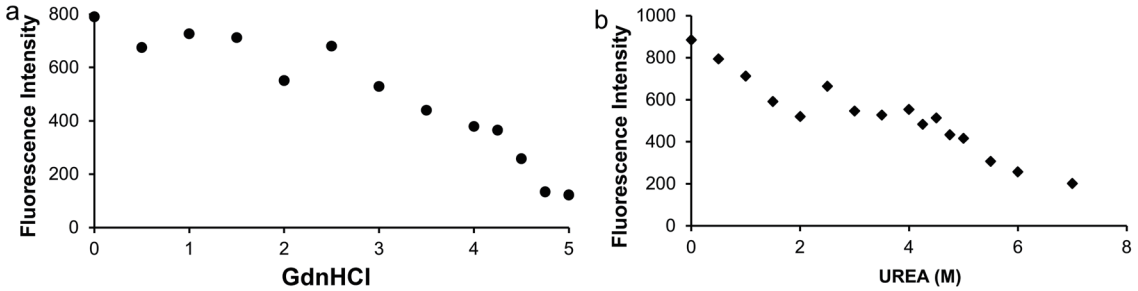

Fig. 3. CRP_{Mt} unfolding and ANS binding. The graph representing ANS binding (represented by the change in fluorescence intensity at 490 nm) at increasing concentrations of (a) GdnHCl and (b) urea. No significant change in fluorescence intensity (increase) was detected due to ANS binding. ANS, 8-anilino-1-napthalenesulphonate; CRP_{Mt}, cyclic adenosine monophosphate receptor protein of *Mycobacterium tuberculosis*; GdnHCl, guanidinium chloride; M, molarity.

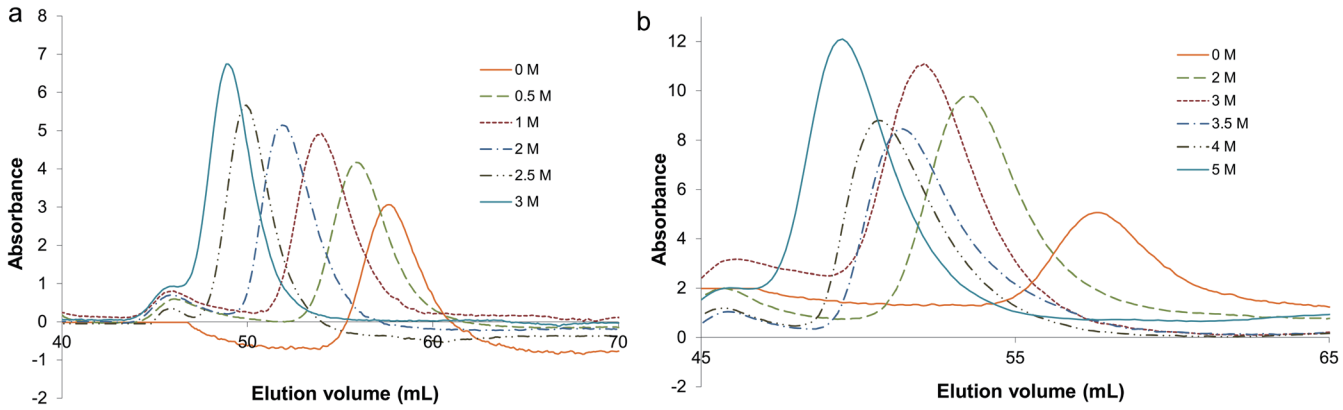

Fig. 4. *CRP*$_{Mt}$ unfolding in the presence of two different chaotropic agents monitored by gel filtration chromatography. Analytical gel filtration chromatography of *CRP*$_{Mt}$ in the presence of varying concentrations of (a) GdnHCl and (b) urea. Protein peaks at a particular urea and GdnHCl concentration were indicated. In all experiments, the same concentration of protein samples (20 μm) was injected into a Superdex S-200 column. *CRP*$_{Mt}$, cyclic adenosine monophosphate receptor protein of *Mycobacterium tuberculosis*; GdnHCl, guanidinium chloride.

HCl- shows good binding to its native promoter region of DNA. The activity of refolded *CRP*$_{Mt}$ was very similar to that of native *CRP*$_{Mt}$ (Fig. S5). This clearly shows regeneration of the structure (domains), function, and DNA binding activity upon refolding, emphasizing the reversible nature of *CRP*$_{Mt}$ unfolding induced by urea or GdnHCl.

Temperature-induced aggregation of CRP$_{Mt}$

It has been observed that *CRP*$_{Mt}$ undergoes irreversible aggregation upon heating. This aggregation leads to the formation of visible precipitation, and the process can be monitored by measuring the light scattering at 360 nm. According to our data, native *CRP*$_{Mt}$ is stable at room temperature, undergoes irreversible unfolding with increasing temperature, and forms aggregate above 60°C temperature. For *CRP*$_{Mt}$, irreversible thermal unfolding starts at 52°C and completes at 65°C along with visible precipitation (Fig. 6).

Discussion

MD simulation of CRP$_{MT}$

To understand the destabilization mechanisms brought upon by temperature, we have performed extensive simulations (50 ns, three replicates or independent simulations at each condition, a total of 150 ns of simulation, Table S2). We started our simulation at room temperature (25°C, normal condition), which provided us insight into the stability of *CRPMt* without any external perturbation factors (*e.g.*, higher temperature or chemical denaturing agents). Figure 7a shows the overall structural deviation of the protein through a change in root mean square deviations (RMSD). The protein at 25°C (control) and 45°C shows similar characteristics in terms of overall structural change, although the RMSD was higher at 45°C. *CRP*$_{Mt}$ structure at 65°C undergoes a large structural alteration. To look at which specific regions were affected by higher temperature, we analyzed root mean square fluctuations averaged over the period for chain A (Fig. 7b). Ignoring the terminal regions (since most proteins are largely flexible at the terminal), we observed peaks of higher fluctuations around residues 50, 100 and 150 in chain A for the control (*CRP*$_{Mt}$ at 25°C) as well as for higher temperatures (45 and 65°C). The changes were almost identical in chains A and B under the same simulation conditions. The protein remains stable when simulated at 25°C (control) and 45°C. Snapshots from the simulation can be seen in supporting data, Figure 8 and S4. In the next section, the unfolding and destabilization of the protein brought about by increasing the temperature to 65°C is discussed in more detail.

Table 3. Elution Volumes of *CRP*$_{Mt}$ at different concentrations of urea and GdnHCl

GdnHCl (M)	Elution volume (mL)	Urea (M)	Elution volume (mL)
0	57.06	0	57.06
0.5	55.87	2.0	53.43
1.0	54.01	3.0	52.12
2.0	51.87	3.5	51.33
2.5	49.94	4.0	50.62
3.0	48.96	5.0	49.5

CRP$_{Mt}$, cyclic adenosine monophosphate receptor protein of *Mycobacterium tuberculosis*; GdnHCl, guanidinium chloride; M, molarity.

Unfolding study of CRP$_{MT}$ *by MD*

The unfolding and destabilization of *CRP*$_{Mt}$ were simulated starting from the crystal structure filled in missing regions (see Methods) at 65°C. Figure 7 displays the global (RMSD) and local (RMSF) structural distortion over time. Figure 8 shows the change in secondary structure composition (in terms of percentage of helices and beta-strands, which also points to the unraveling of the overall structure at higher temperatures. Figure 9 displays the local unfolding and destabilizing at higher temperatures at different snapshots during the simulation. At 65°C, the structure collapses within 10 ns of the simulation. Notably, the interface region is distorted, but since the structure collapses, it forms a more artificially compact structure (the buried surface area increased from 1,339 to 1,845 Å^2, Figure S6). Notably, the secondary structures were not equally affected by higher temperatures, and the alpha-helices degraded faster than the beta-sheets (helicity reduces from 37 to 33%, and strand composition reduces from 25 to 22% at 65°C). Changes in secondary structural composition over time can be seen in Figure 9, which points

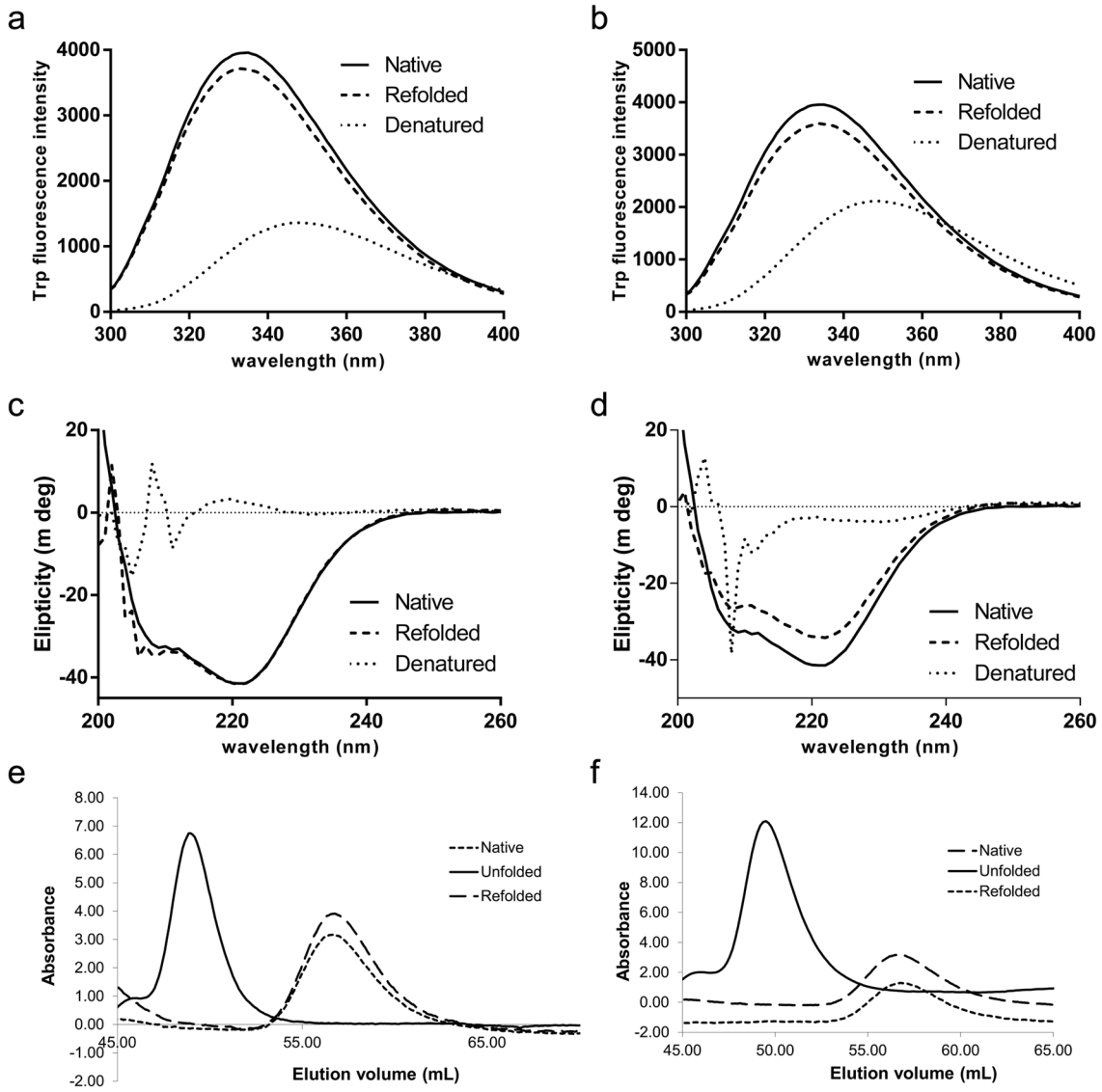

Fig. 5. Equilibrium Unfolding of CRP_{Mt} was reversible. GdnHCl-denatured (a, c, and e) and urea-denatured (b, d, and f) proteins were successfully refolded, and protein refolding was monitored by various biophysical techniques. CRP_{Mt}, cyclic adenosine monophosphate receptor protein of *Mycobacterium tuberculosis*; GdnHCl, guanidinium chloride.

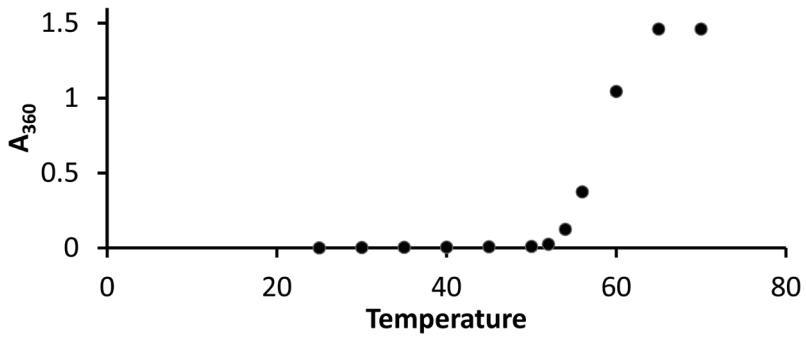

Fig. 6. Temperature-induced irreversible aggregation of CRP_{Mt}. The protein (in buffer A) was heated at increasing temperatures, and aggregation was monitored using static light scattering in a spectrofluorometer. CRP_{Mt}, cyclic adenosine monophosphate receptor protein of *Mycobacterium tuberculosis*.

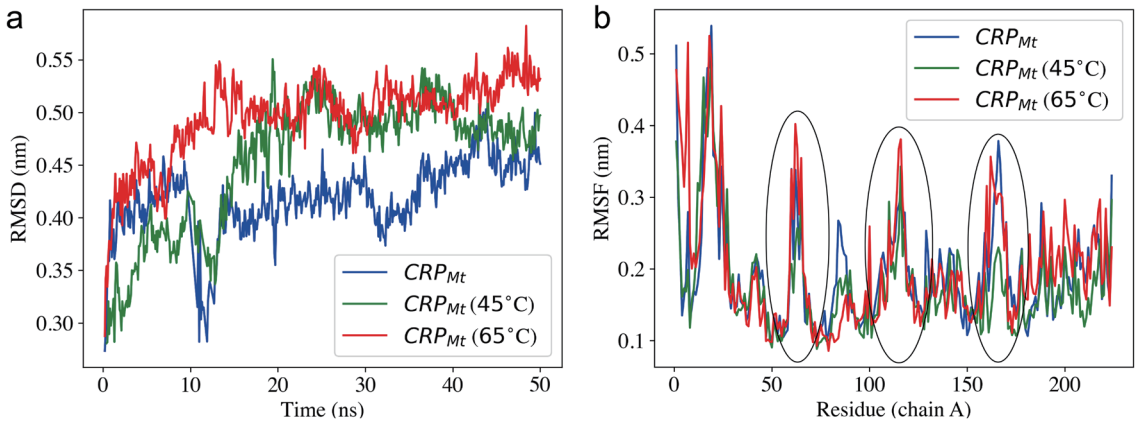

Fig. 7. Structural deviations observed during simulations, comparing CRP_{Mt} at room temperature with the protein at two different temperatures (45 and 65°C), using (a) Root mean square deviations (RMSD) vs. time (shows the overall structural deviations) and (b) Root mean square fluctuations (RMSF) for each residue in chain A. Regions of high fluctuations are encircled, highlighting the regions in the protein that undergo significant local changes due to temperature changes. CRP_{Mt}, cyclic adenosine monophosphate receptor protein of *Mycobacterium tuberculosis*.

to distortion of secondary structural elements due to the effect of higher temperature. Hydrogen bonding patterns were also affected; the contacts prevalent in the control (Table S3) were not found at higher temperatures (the pairs not highlighted as bold are only present at the specific condition).

Overall distortions of the protein were only pronounced at higher temperatures; all the parameters reflect the same trend (Fig. 7). Larger fluctuations were also observed for CRP_{Mt} at 65°C. The interface of the native protein has two helices crossed over each other (see first structure in Fig. 8); this interaction was gradually lost at 65°C, and this phenomenon was also visible in the change in the buried surface of the complex over time (Fig. S7).

Conclusion

In this study, we extensively examined the folding and unfolding transition of a crucial transcription regulator protein in *Mycobacterium tuberculosis*. Both experimental and computational analyses suggest that CRP is stable at room temperature. However, it begins to unfold under elevated temperature or increasing denaturant conditions. We

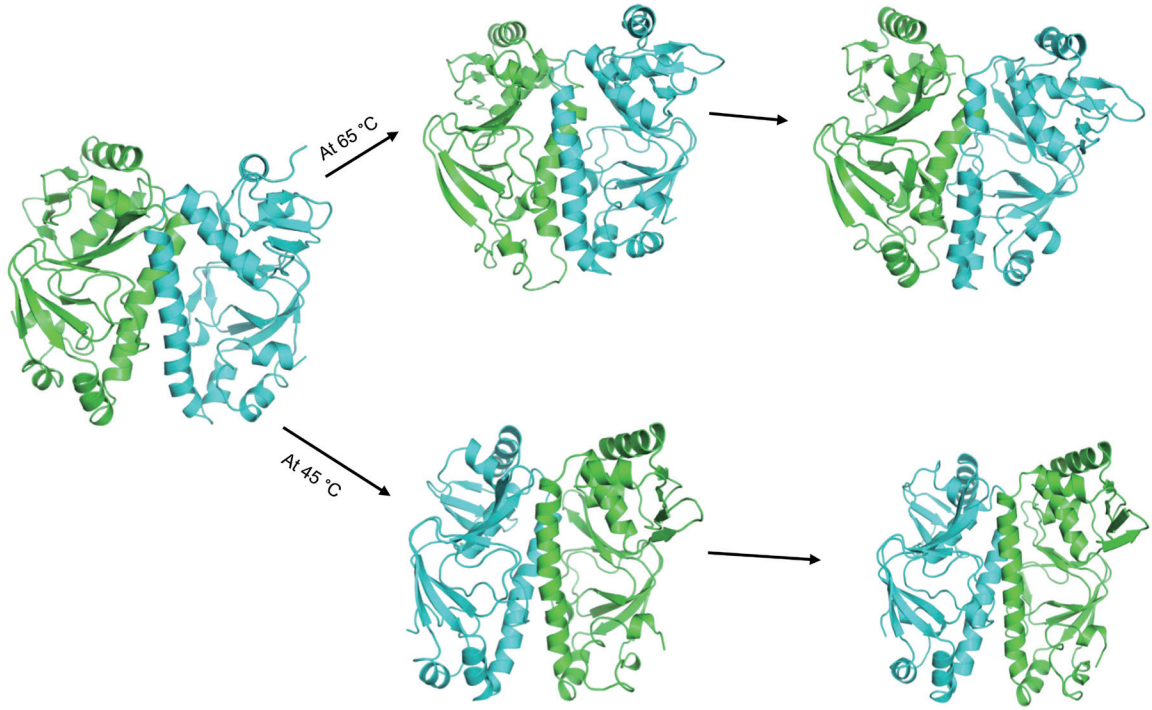

Fig. 8. Snapshots of CRP_{Mt} showing local unfolding and destabilizing at higher temperatures. The two chains are shown in green and cyan cartoons. The starting structure was taken from the control (at 25°C), showing the distortion of the complex at higher temperatures during the simulation, especially around the interface. CRP_{Mt}, cyclic adenosine monophosphate receptor protein of *Mycobacterium tuberculosis*.

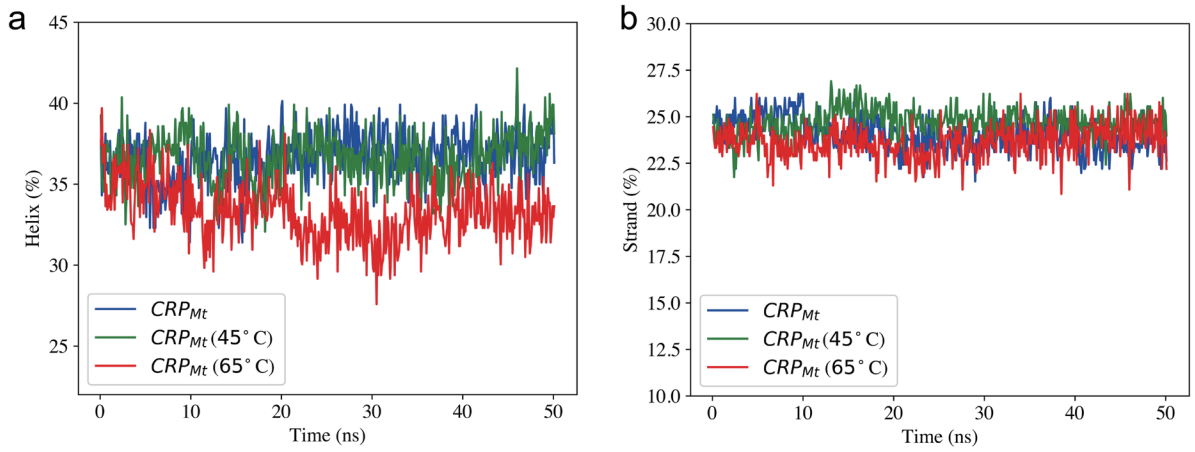

Fig. 9. Change in secondary structure composition during simulation. (a) Percentage helicity vs. time and (b) Percentage strands vs. time for CRP_{Mt} at room temperature (blue) and higher temperatures (45 and 65°C). During the simulation, ~5% reduction in helicity content and 3% reduction in beta-strands were observed at 65°C. CRP_{Mt}, cyclic adenosine monophosphate receptor protein of *Mycobacterium tuberculosis*.

observed that the unfolding induced by urea and GdnHCl is highly reversible. Once the denaturant is removed from the medium, the protein automatically reverts to its native conformation. Conversely, we found that temperature-mediated unfolding of CRP is irreversible, with the protein forming visible aggregates at higher temperatures. Our computational analysis further corroborates our experimental observations and identifies the region of the protein responsible for unfolding. Overall, this study provides a comprehensive understanding of CRP's structural rearrangements during the folding/unfolding process, which may have significant implications for the design of next-generation therapeutics against *Mycobacterium.*

Acknowledgments

The authors would like to thank Prof. Pradeep Parrack of Bose Institute for his overall help in completing this study.

Funding

SC was funded by the Homing program of the Foundation for Polish Science, co-financed by the European Union under the European Regional Development Fund, grant No. Homing/2017-3/22. SC was also funded by the Ramalingaswami Fellowship (BT/RLF/Re-entry/09/2019) awarded by the Department of Biotechnology, India.

Conflict of interest

SC has been an editorial board member of *Gene Expression* since June 2023. The other authors have no other conflict of interests to declare.

Author contributions

AS carried out experiments, analyzed data, and wrote the manuscript. DC performed molecular dynamics simulation and computational analysis, analyzed the data, and wrote the manuscript. SC conceived the idea, analyzed data, oversaw the work, and wrote the manuscript. All authors contributed to writing the manuscript.

Data sharing statement

All the raw data and other materials are available from the corresponding author upon reasonable request.

References

[1] Khan H, Paul P, Sevalkar RR, Kachhap S, Singh B, Sarkar D. Convergence of two global regulators to coordinate expression of essential virulence determinants of Mycobacterium tuberculosis. Elife 2022;11:e80965. doi:10.7554/eLife.80965, PMID:36350294.

[2] Stapleton M, Haq I, Hunt DM, Arnvig KB, Artymiuk PJ, Buxton RS, *et al*. Mycobacterium tuberculosis cAMP receptor protein (Rv3676) differs from the Escherichia coli paradigm in its cAMP binding and DNA binding properties and transcription activation properties. J Biol Chem 2010;285(10):7016–7027. doi:10.1074/jbc.M109.047720, PMID:20028978.

[3] Zhou J, Lv J, Carlson C, Liu H, Wang H, Xu T, *et al*. Trained immunity contributes to the prevention of Mycobacterium tuberculosis infection, a novel role of autophagy. Emerg Microbes Infect 2021;10(1):578–588. doi:10.1080/22221751.2021.1899771, PMID:33666534.

[4] Di Y, Xu S, Chi M, Hu Y, Zhang X, Wang H, *et al*. Acetylation of cyclic AMP receptor protein by acetyl phosphate modulates mycobacterial virulence. Microbiol Spectr 2023;11(1):e0400222. doi:10.1128/spectrum.04002-22, PMID:36700638.

[5] Gárate F, Dokas S, Lanfranco MF, Canavan C, Wang I, Correia JJ, *et al*. cAMP is an allosteric modulator of DNA-binding specificity in the cAMP receptor protein from Mycobacterium tuberculosis. J Biol Chem 2021;296:100480. doi:10.1016/j.jbc.2021.100480, PMID:33640453.

[6] Ni Z, Cheng X. Origin and isoform specific functions of exchange proteins directly activated by cAMP: A phylogenetic analysis. Cells 2021;10(10):2750. doi:10.3390/cells10102750, PMID:34685730.

[7] Körner H, Sofia HJ, Zumft WG. Phylogeny of the bacterial superfamily of Crp-Fnr transcription regulators: exploiting the metabolic spectrum by controlling alternative gene programs. FEMS Microbiol Rev 2003;27(5):559–592. doi:10.1016/S0168-6445(03)00066-4, PMID:14638413.

[8] Youn H, Carranza M. cAMP activation of the cAMP receptor protein, a model bacterial transcription factor. J Microbiol 2023;61(3):277–287. doi:10.1007/s12275-023-00028-6, PMID:36892777.

[9] Green J, Stapleton MR, Smith LJ, Artymiuk PJ, Kahramanoglou C, Hunt DM, *et al*. Cyclic-AMP and bacterial cyclic-AMP receptor proteins revisited: adaptation for different ecological niches. Curr Opin Microbiol 2014;18(100):1–7. doi:10.1016/j.mib.2014.01.003, PMID:24509484.

[10] Rickman L, Scott C, Hunt DM, Hutchinson T, Menéndez MC, Whalan R, *et al*. A member of the cAMP receptor protein family of transcription regulators in Mycobacterium tuberculosis is required for virulence in mice and controls transcription of the rpfA gene coding for a resuscitation promoting factor. Mol Microbiol 2005;56(5):1274–1286. doi:10.1111/j.1365-2958.2005.04609.x, PMID:15882420.

[11] Reddy MCM, Palaninathan SK, Bruning JB, Thurman C, Smith D, Sacchettini JC. Structural insights into the mechanism of the allosteric transitions of Mycobacterium tuberculosis cAMP receptor protein. J Biol Chem 2009;284(52):36581–36591. doi:10.1074/jbc.M109.041343, PMID:19740754.

[12] Kumar P, Joshi DC, Akif M, Akhter Y, Hasnain SE, Mande SC. Mapping conformational transitions in cyclic AMP receptor protein: crystal structure and normal-mode analysis of Mycobacterium tuberculosis apo-cAMP receptor protein. Biophys J 2010;98(2):305–314. doi:10.1016/j.bpj.2009.10.016, PMID:20338852.

[13] Gallagher DT, Smith N, Kim SK, Robinson H, Reddy PT. Profound asymmetry in the structure of the cAMP-free cAMP receptor protein (CRP) from mycobacterium tuberculosis. J Biol Chem 2009;284(13):8228–8232. doi:10.1074/jbc.C800215200, PMID:19193643.

[14] Kahramanoglou C, Cortes T, Matange N, Hunt DM, Visweswariah SS, Young DB, *et al*. Genomic mapping of cAMP receptor protein (CRP Mt) in Mycobacterium tuberculosis: relation to transcriptional start sites and the role of CRPMt as a transcription factor. Nucleic Acids Res 2014;42(13):8320–8329. doi:10.1093/nar/gku548, PMID:24957601.

[15] Bai G, McCue LA, McDonough KA. Characterization of mycobacterium tuberculosis Rv3676 (CRPMt), a cyclic AMP receptor protein-like DNA binding protein. J Bacteriol 2005;187(22):7795–7804. doi:10.1128/JB.187.22.7795-7804.2005, PMID:16267303.

[16] Mirny LA. Chromosome and protein folding: In search for unified principles. Curr Opin Struct Biol 2023;81:102610. doi:10.1016/j.sbi.2023.102610, PMID:37327690.

[17] Dishman AF, Volkman BF. Metamorphic protein folding as evolutionary adaptation. Trends Biochem Sci 2023;48(8):665–672. doi:10.1016/j.tibs.2023.05.001, PMID:37270322.

[18] Moghadam SK, Toroghi SE, Vatanparast MK, Jouyaeian P, Mokaberi P, Yazdyani H, *et al*. Novel perspective into the interaction behavior study of the cyanidin with human serum albumin-holo transferrin complex: Spectroscopic, calorimetric and molecular modeling approaches. J Mol Liq 2022;356:119042. doi:10.1016/j.molliq.2022.119042.

[19] Zare-Feizabadi N, Amiri-Tehranizadeh Z, Sharifi-Rad A, Mokaberi P, Nosrati N, Hashemzadeh F, *et al*. Determining the interaction behavior of calf thymus DNA with anastrozole in the presence of Histone H1: spectroscopies and cell viability of MCF-7 cell line investigations. DNA Cell Biol 2021;40(8):1039–1051. doi:10.1089/dna.2021.0052, PMID:34165362.

[20] Assaran Darban R, Shareghi B, Asoodeh A, Chamani J. Multi-spectroscopic and molecular modeling studies of interaction between two different angiotensin I converting enzyme inhibitory peptides from gluten hydrolysate and human serum albumin. J Biomol Struct Dyn 2017;35(16):3648–3662. doi:10.1080/07391102.2016.1264892, PMID:27897084.

[21] Alaei L, Ashengroph M, Moosavi-Movahedi AA. The concept of protein folding/unfolding and its impacts on human health. Adv Protein Chem Struct Biol 2021;126:227–278. doi:10.1016/bs.apcsb.2021.01.007, PMID:34090616.

[22] Acharya N, Jha SK. Dry molten globule-like intermediates in protein folding, function, and disease. J Phys Chem B 2022;126(43):8614–8622. doi:10.1021/acs.jpcb.2c04991, PMID:36286394.

[23] Jing W, Qin Y, Tong J. Effects of macromolecular crowding on the folding and aggregation of glycosylated MUC5AC. Biochem Biophys Res Commun 2020;529(4):984–990. doi:10.1016/j.bbrc.2020.06.156, PMID:32819609.

[24] Datta AB, Roy S, Parrack P. Disorder-order transition of lambda CII promoted by low concentrations of guanidine hydrochloride suggests a stable core and a flexible C-terminus. Eur J Biochem 2003;270(22):4439–4446. doi:10.1046/j.1432-1033.2003.03835.x, PMID:14622272.

[25] Lakowicz JR, editor. Principles of fluorescence spectroscopy. 2nd ed. New York: Kluwer Academic/Plenum; 1999. doi:10.1007/978-1-4757-3061-6.

[26] Malek-Esfandiari Z, Rezvani-Noghani A, Sohrabi T, Mokaberi P, Amiri-Tehranizadeh Z, Chamani J. Molecular Dynamics and Multi-Spectroscopic of the Interaction Behavior between Bladder Cancer Cells and Calf Thymus DNA with Rebeccamycin: Apoptosis through the Down Regulation of PI3K/AKT Signaling Pathway. J Fluoresc 2023;33(4):1537–1557. doi:10.1007/s10895-023-03169-4, PMID:36787038.

[27] Pace CN, Shaw KL. Linear extrapolation method of analyzing solvent denaturation curves. Proteins 2000;41(Suppl 4):1–7. doi:10.1002/1097-0134(2000)41:4+<1::aid-prot10>3.3.co;2-u, PMID:11013396.

[28] Chakrabarty SP, Balaram H. Reversible binding of zinc in Plasmodium falciparum Sir2: structure and activity of the apoenzyme. Biochim Biophys Acta 2010;1804(9):1743–1750. doi:10.1016/j.bbapap.2010.06.010, PMID:20601220.

[29] Mukherjee D, Pal A, Chakravarty D, Chakrabarti P. Identification of the target DNA sequence and characterization of DNA binding features of HlyU, and suggestion of a redox switch for hlyA expression in the human pathogen Vibrio cholerae from in silico studies. Nucleic Acids Res 2015;43(3):1407–1417. doi:10.1093/nar/gku1319, PMID:25605793.

[30] Webb B, Sali A. Comparative protein structure modeling using MODELLER. Curr Protoc Bioinformatics 2016;54:5.6.1–5.6.37. doi:10.1002/cpbi.3, PMID:27322406.

[31] Van Der Spoel D, Lindahl E, Hess B, Groenhof G, Mark AE, Berendsen HJ. GROMACS: fast, flexible, and free. J Comput Chem 2005;26(16):1701–1718. doi:10.1002/jcc.20291, PMID:16211538.

[32] Kaminski GA, Friesner RA, Tirado-Rives J, Jorgensen WL. Evaluation and reparametrization of the OPLS-AA force field for proteins via comparison with accurate quantum chemical calculations on peptides. The Journal of Physical Chemistry B 2001;105(28):6474–6487. doi:10.1021/jp003919d.

[33] Petersen CF, Searles DJ. Equilibrium distribution functions: connection with microscopic dynamics. Phys Chem Chem Phys 2022;24(11):6383–6392. doi:10.1039/d1cp05316g, PMID:35262116.

[34] Chatterjee T, Chakraborti S, Joshi P, Singh SP, Gupta V, Chakrabarti P. The effect of zinc oxide nanoparticles on the structure of the periplasmic domain of the Vibrio cholerae ToxR protein. FEBS J 2010;277(20):4184–4194. doi:10.1111/j.1742-4658.2010.07807.x, PMID:20825484.

[35] Suryawanshi VD, Walekar LS, Gore AH, Anbhule PV, Kolekar GB. Spectroscopic analysis on the binding interaction of biologically active pyrimidine derivative with bovine serum albumin. J Pharm Anal 2016;6(1):56–63. doi:10.1016/j.jpha.2015.07.001, PMID:29403963.